Journal of the Nigerian Association of Mathematical Physics
Volume 26, (*March, 2014*), pp 177 – 186

Ab Initio Study of the Electronic Structure of Silicon Quantum DOTS

Sylvester A. Ekong†[1], I. A. Fuwape[2], and E. A. Odo[2]

[1]Department of Physics and Energy Studies,
Achievers University, Owo, Nigeria
[2]Department of Physics,
Federal University of Technology, Akure, Nigeria

Abstract

In this work, first principle calculation was performed on three nanostructures of hydrogenterminated silicon quantum dots namely: (a) Si_5H_{12} ***(b)*** Si_8H_{11} ***and (c)*** $Si_{16}H_{20}$ ***.Calculations on structural relaxation using DFT self-consistent total energy scheme with a convergence criterion of the Hellman-Feynman forces set at 1meV/Å; and plane wave basis with kinetic energycut-off energy of 35Ry integrated over a Brilloun zone of uniform grid of 5x5x5 points was also performed .The variation of the ground state total system energy with the planewavecutoff energy, K–Points, and lattice constant were graphically analysed. The results obtained shows that the ground state total system energy have a local minimum for a range of theplanewavecutoff energy, K–points, and lattice parameter values. The Si–Si and Si–H bond lengths are approximately structurally size independent; whereas the bond angles appear to have small size dependence. Also, the lattice parameter and equilibrium volume increases linearly with molecular size; whereas the bulk modulus and equilibrium energy decreases with increasing size of the silicon quantum dots. The band structure calculation reveals distinctively, a discretization of energy levels in the band structure due to quantum confinement as well as a shift from the indirect HOMO–LUMO energy gap found in bulk silicon to a direct one. The size of the energy gap was also observed to decrease with increasing quantum dot size.Furthermore, the results obtained in this work are in good agreement with other theoretical quantum dot models as well as those obtainedfrom experimental data, showing that this model can be used to predict both structural and electronic properties of silicon quantum dots in this size range.***

Keywords: Supercell, QD, HOMO, LUMO, Geometrically optimized structures

1.0 Introduction

Low-dimensional nanometer-sized systems have defined a new research area in condensed-matter physics within the last 20 years.The nanocrystalline silicon (nc-Si) is extremely investigated, not only because of its various applications, but also because of the interest presented by new phenomena that takes place at nanometric scale [1, 2]. Siliconhas emerged as a dominant material from the dawn of microelectronics back in 1950-s [3] andit still remains the heart of all modern microelectronics. Its properties have allowed the semiconductor industry to follow Moore's law for nearly half a century; and remarkably silicon is an ideal material to manipulate quantum information encoded in individual electrons [4]. In the case of the nanocrystalline silicon (nc-Si), quantum confinement is dominant in transport processes and has an important contribution in their electronic phenomena. Silicon nanocrystalline properties which are derived from this effect, are very sensitive to shape and size [3, 4, 5, 6, and 7] distributions within the sample. It is therefore important to control this size with a maximum accuracy. Nanocrystalline silicon (nc-Si), is obviously compatible with the classical silicon-based devices [8].

According to (IlyaSychugov, 2006), a recent article by 2016 inventive new device architecturesmay well take silicon electronics comfortably into the regime where components are smallerthan 10 nm. On top of the related problems with existing crystal-growth methods, currentinsulating materials and defect control, new physical effects are coming onto the scene. Atthis range of sizes purely quantum effects, such as quantum confinement, become significant.The quantum mechanical effects may impose insurmountable problems for future devices butmay, just as well, provide new pathways. The

Corresponding author: ***Sylvester A. Ekong,*** E-mail: ani_sly@yahoo.co.uk, Tel.: +2348034968173

quantum confinement effect, being a direct confirmation of elementary quantummechanics and the Schrodinger equation, has been widely investigated in direct bandgapnanocrystals due to their straightforward optical applications. This research field goes back tothe beginning of the 1980-s, when the theoretical background was put forward. Nowadayssome quantum dot [3] related devices, such as lasers, can compete on equal terms with otherdesigns for occupying a niche in the market.

These two major semiconductor topics, silicon and nanocrystals, started merging togetherwith the prospect of application in optoelectronics in the beginning of the 1990-s, fostering astrong interest in the research community. First in the form of nanoporous silicon, then asnanocrystals (or, for amorphous phase, nanoclusters) embedded in a silicon dioxide matrix.Although the on-chip laser appeared to be more difficult to reach than first anticipated, otherunforeseen applications, including ones in biology gradually emerged.

The construction of supercell for silicon quantum dots and investigating their size dependent electronic band structures on single-dot level in order to reveal the basic mechanism of its electronic properties is the main goal of the present work.

2.0 Methodology

2.1 Computational Methods

In this work, 3 types of silicon based quantum dots were constructed consisting of (a) five atoms of silicon, (b) eight atoms of silicon and (c) sixteen atoms of silicon. To model the molecules, a periodic arrangement of simple cubic *sc*supercells, starting with an ideal diamond lattice structure of bulk silicon was used. The supercell was made large enough to avoid interactions between the molecule and its images.

In the case of structure (a), the two main atoms of the primitive lattice structure of bulk silicon were repeated in a 1x1x2 supercell to construct a five atoms structure. For the structure (b), the eight atoms constituting the FCC diamond structure unit cell of bulk silicon was used as the starting supercell structure. For the structure (c) with sixteen atoms, the FCC unit cell of silicon of (b) was repeated in the z direction as a 1 x 1 x 2 supercell structure.

For each of the constructed structures, structurally relaxed electronic ground states of the considered molecules were determined by DFT total-energy simulation using a large simple cubic structure of dimension greater than the initial size of the atoms in the different structures. The convergence criterion for the Hellmann-Feynman forces was set to $1meV$ /Å. After this initial structural minimization process, all the dangling bonds associated with the silicon atoms were terminated with hydrogen and the structural optimization process was repeated for the three new structures represented here as (a) Si_5H_{12} (b) Si_8H_{11} and (c) $Si_{16}H_{20}$.

For the different structures, the LDA functional in the Perdew-Zunger parameterization was used to model the exchange-correlation effects for both the silicon and hydrogen atoms constituting each structure. The electron-ion interaction is described by first-principlesnorm-conserving pseudopotentials that have been generated within the Hamann scheme. To ensure optimization of the lattice parameter of the different structures, a usual practice of computing the ground state energy of the system by first varying the plane wave energy cutoff for a constant K-points distribution and vice-versa, followed by variation of the lattice parameter in the quantum espresso input file was performed. A plane wave basis set for the electronic wave functions with a kinetic energy cutoff of 35 Ry and a Brillouin zone with a uniform grid of 5×5×5 points were determined as being suitable for the convergence of the calculation with consideration on the limited computational power. These values were used in all the calculations as well as in determining the size (lattice constant) of the final stable atomic structure of each quantum dot.

The different calculations that were performed on the structures apart from the initial structural relaxation calculations included, the self-consistence (scf) ground state energy and the norm-conserving band structure calculations, from which important characteristics like the distribution and shape of the energy bands as well as the energy difference between the lowest unoccupied molecular orbital (LUMO) and the highest occupied molecular orbital (HOMO) were derived.

The volume of a cluster can be approximately define by (Gong, 1995),

$$V = \frac{4}{3}\pi R_o^3, \tag{1}$$

where R_o is the radius of the cluster [9], and can be related to the bulk modulus of the materials as (Sholl and Steckel, 2009)

$$B_o = \frac{V\partial^2 E_{tot}}{\partial V^2} \tag{2}$$

where the derivative is evaluated at the equilibrium lattice parameter [10].

A more detailed mathematical treatment with an equation of state that relates the two quantities in equation (1) and (2) over a wider range of lattice constants ‘a’, is the well-known Birch–Murnaghan equation of state for isotropic solids given as (Francis Birch, 1947),

$$E_{tot}(a) = E_o + \frac{9V_oB_o}{16}\left\{\left[\left(\frac{a_o}{a}\right)^{2/3} - 1\right]^3 B_o' + \left[\left(\frac{a_o}{a}\right)^{2/3} - 1\right]^2\left[6 - 4\left(\frac{a_o}{a}\right)^{2/3}\right]^3\right\} \quad (3)$$

In this expression, a_o is the equilibrium lattice constant, V_o is the equilibrium volume per atom, B_o is the bulk modulus at zero pressure, $P = 0$, and $B_o' = \left(\partial B / \partial P\right)_T$.

3.0 Results and Discussion

3.1 Structural Optimization of the quantum dots

The structures of the three types of hydrogen-terminated silicon quantum dot were modeled in supercells. Figure 1 shows the geometrically optimized structure for the (a) Si_5H_{12} (b) Si_8H_{11} and (c) $Si_{16}H_{20}$ molecules, which ensure that the inter-atomic forces were smaller than $1meV$ /Å.

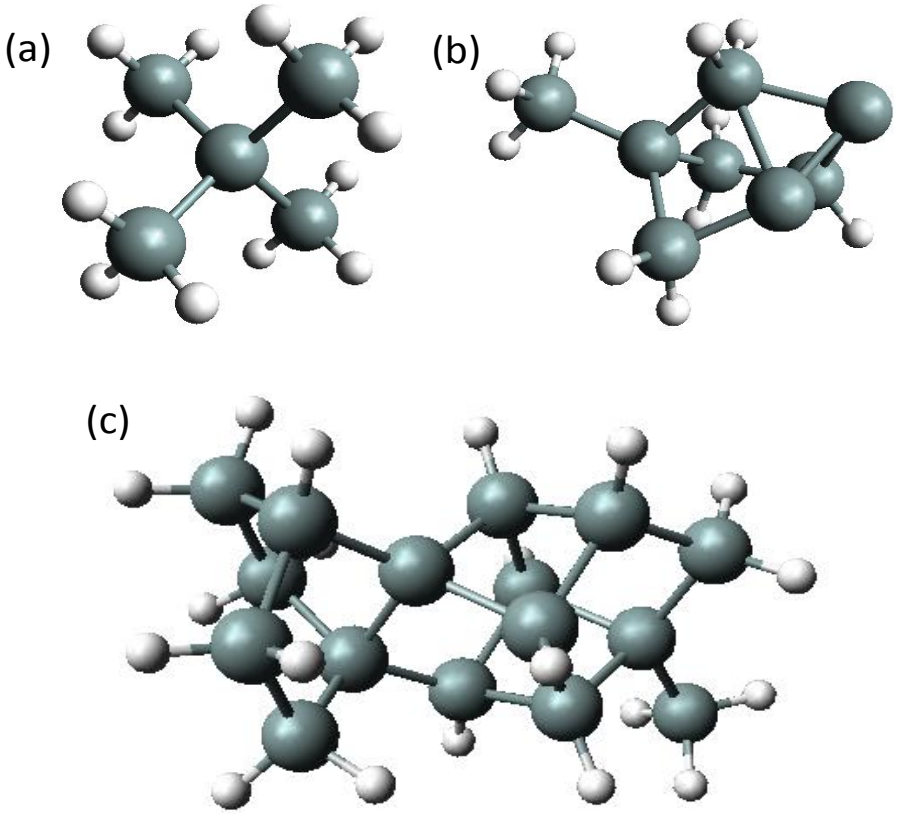

Figure 1: Geometrically optimized structure for (a) Si_5H_{12} (b) Si_8H_{11} and (c) $Si_{16}H_{20}$ molecules.

Table 1:Quantum Dots and their average bond lengths and bond angles

Molecule	Average Si-Si Bond length	Average Si-Si-Si Bond angle	Average Si-H bond length
Si_5H_{12}	$2.34\,\text{Å}^o$	109.70^o	$1.42\,\text{Å}^o$
Si_8H_{11}	$2.38\,\text{Å}^o$	92.06^o	$1.42\,\text{Å}^o$
$Si_{16}H_{20}$	$2.36\,\text{Å}^o$	107.81^o	$1.42\,\text{Å}^o$

Table 1, shows the molecular properties of the final relaxed structures with the surface dangling bonds of the silicon atoms passivated by hydrogen atoms. The $Si-Si$ atoms bond distribution length in all the three structures considered have an average form comparable to the $2.35\,\text{Å}^o$ nearest-neighbor distance of bulk silicon [11]. This is a good indicator that the

induced lattice straining was minimal in all three structures studied [12]. The average $Si-Si$ atoms bond angle however, varied by as much as 18^o from the 109.5^o of standard strain free bulk silicon in the case of the Si_8H_{11}. The two other structures, namely the Si_5H_{12} and the $Si_{16}H_{20}$ have bond angles in the expected range. The bond length of the surface termination hydrogen atom to the silicon maintained a stable value of $1.42\,\mathring{A}$.

Figures 2 and 3, shows the plot of the total system energy-calculation with respect to cutoff energy for first-principle (DFT) based calculations and the convergence of total system energies with respect to k-points for the system Si_5H_{12} respectively. The arrows on the plots points to suitable minimum values of the plane wave cutoff energy as 35Ry and a Monkhorst-park k-points mesh density of 5×5×5 respectively. These values are sufficient for convergence in the calculation of the structure properties of the nanoclusters used in this study.

Since many of the properties of nanomaterials including nanoparticles depend largely on their size parameter, an attempt was done to estimate the lattice parameter and hence compressibility of the final relaxed structures. Figure 4, shows the plot of the variation of the total system energy (squared points) as a function of the lattice parameter near the equilibrium lattice for the Si_5H_{12} quantum dot structure as an example.

The results of fitting the equation of state (in equation 3 above) to the full set of the calculated data is as shown in Figure 1, for the Si_5H_{12} structure resulted in the values $a_o = 11.0(a.u.) = 5.82\,\mathring{A}$ and $B_o = 16.4GPa$. Table 2 shows the different structural parameter as well the ground state energy for the three quantum dot structures studied in this work.

Table 2:Quantum Dots with their Bulk modulus, Equilibrium volume and energy

Molecule	**Lattice parameter** a_o	**Bulk Modulus** B_o	**Equilibrium Volume** V_o	**Equilibrium Energy** E_o
Si_5H_{12}	$5.82\,\mathring{A}$	$16.4GPa$	$197.26\,\mathring{A}^3$	$-53.29(Ry)$
Si_8H_{11}	$7.41\,\mathring{A}$	$15.4GPa$	$406.62\,\mathring{A}^3$	$-74.47(Ry)$
$Si_{16}H_{20}$	$11.13\,\mathring{A}$	$13.4GPa$	$1378.75\,\mathring{A}^3$	$-149.67(Ry)$

From the table, there is an obvious increase in the cluster sizes with increasing number of atomic elements constituting the different structures as indicated in the column under lattice parameters. Again, a similar increase is noticeable in the equilibrium volume, with decreasing ground state energy of the system. The equilibrium lattice parameters in all the cases represents the size of the cubicle needed to contain the atoms of each structure; and thus can be taken as the numbers for the diameter of the different quantum dots. While the trend exhibited with the lattice parameter of the structures is obvious, the decrease of the bulk modulus values with increasing size of the structure is not very clear, (a possible reason could be based on the number of dangling bonds passivated in each structure by the hydrogen atom for which the structure Si_5H_{12} have more dangling bonds passivated; this reasoning may be investigated further) however their small bulk modulus values in the range $13-16GPa$ when compare to the $101GPa$ for bulk silicon is an indication of a relatively high compressibility values for the quantum dot structures.

Nanomaterials, including nanoparticles have been found to exhibit different physical, chemical, and mechanical properties from the corresponding bulk materials. The melting temperature and the thermal conductivity decreases significantly in nanocrystals compared to their respecting bulk. The changes associated with the elasticity and the vibrational characterization of nanomaterials is related to the surface effect resulting from the high surface to volume ratio of nanomaterial [13]. The small values of the bulk modulus in these structures are indication of relatively small cohesive forces holding the atoms of the structures together. Hence, these structures will exhibit low melting temperatures and other physical property changes associated with nanoparticles.

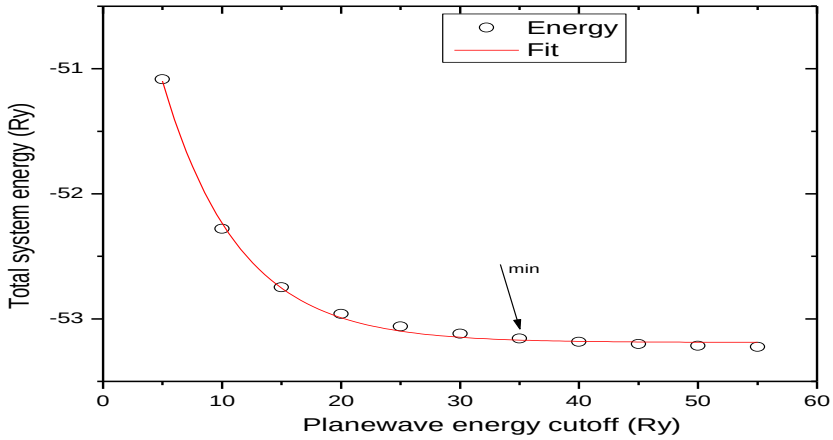

Figure 2: A Plot of the Variation of the Total System Energy with Planewave Energy Cutoff.

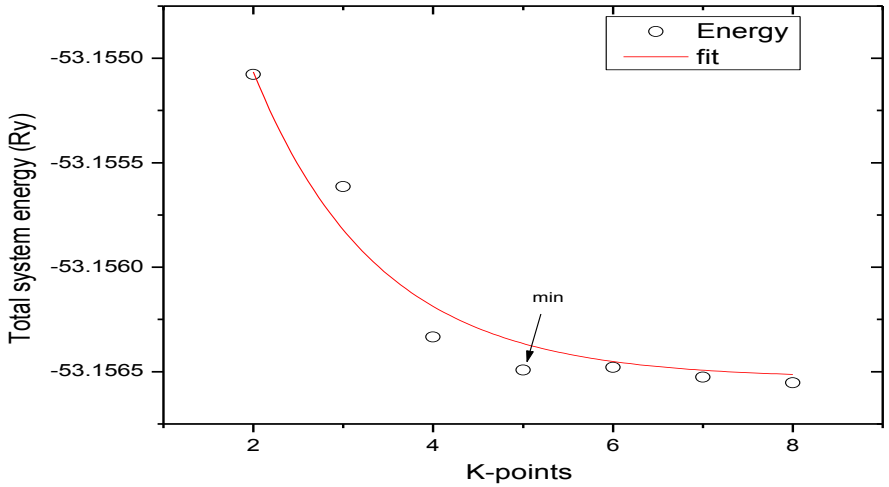

Figure 3: A Plot of the Variation of the Total System Energy with K–Points.

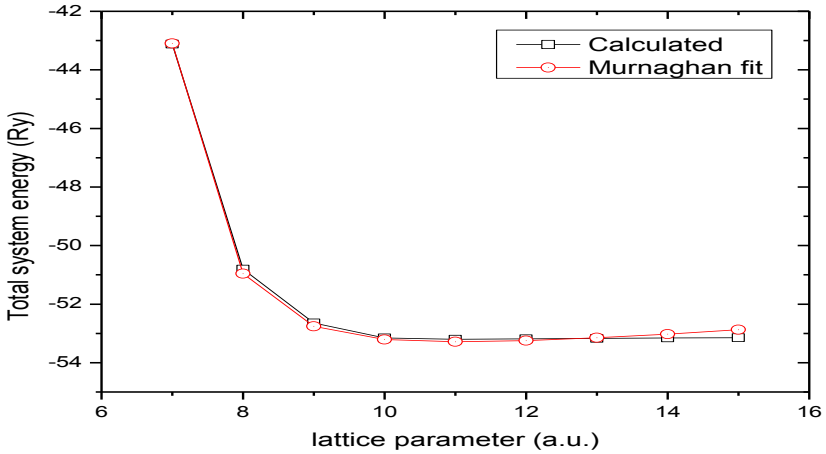

Figure 4: A Plot of the Variation of the Total System Energy with Lattice Parameter.

3.2 Electronic band structure

Figure 5 shows the electronic band structure of bulk silicon with lattice constant of $5.43\overset{o}{\text{A}}$, calculated using the quantum espresso code for comparison purpose. The top of the valence band or highest occupied molecular orbital (HOMO) lies at the $\Gamma(0.0, 0.0, 0.0)$ symmetry point in the Brillioun zone, considered as the zero point energy. The conduction band minimum or lowest unoccupied molecular orbital (LUMO) on the other hand, appears near the X -symmetry point at $k_x = 0.46$; such misalignment in the point of occurrence of the HOMO and LUMO level is responsible for the resulting indirect band gap properties exhibited by bulk silicon [14]. The difference between the LUMO and HOMO levels, gives an indirect band gap value of $0.645eV$ which is about 40% underestimation of experimental band gap of bulk silicon. This is due to the discontinuity in the exchange-correlation potential upon the addition of an electron. In practice the computed band gap values in plane-wave pseudopotential DFT calculations are usually compensated [14]. The discontinuity has been calculated to be $0.58eV$, and the calculated band gaps will be less than actual values by this amount [15].

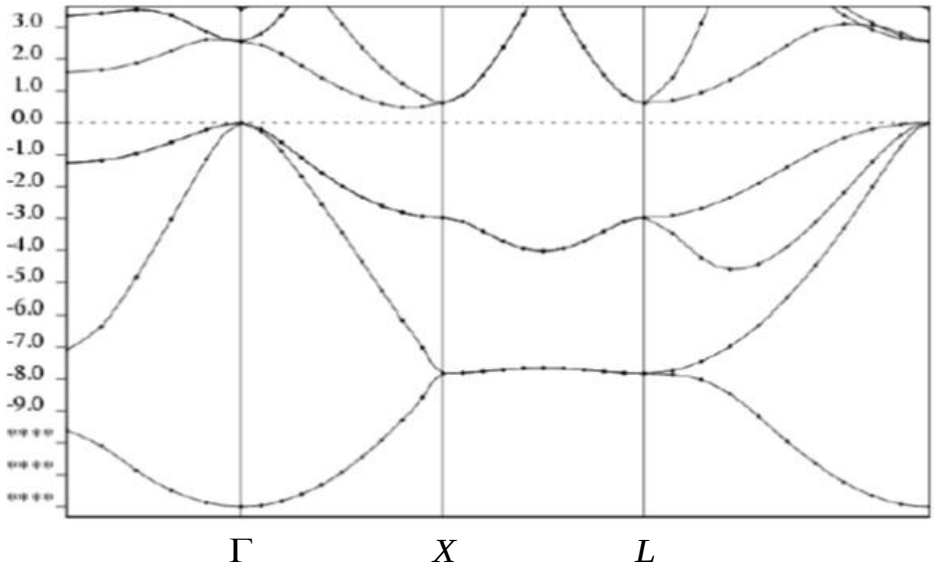

Figure 5: The Variation of Electronic Band Gap Structure of Bulk Silicon with Lattice Constant.

With this in the background DFT calculations are performed within the generalized gradient approximation (GGA) to determination the electronic properties of the three silicon quantum dots structures whose structural properties were discussed earlier.

Figures 6, 7 and 8 shows the electronic band structures for the fully relaxed structures of the (a) Si_5H_{12} (b) Si_8H_{11} and (c) $Si_{16}H_{20}$ molecules respectively. One obvious difference between the band structures of the quantum dots when compared with the band structure of bulk silicon in Figure 5 is the well separated and fairly constant band levels in both the conduction and valence bands. Such distinct band levels have been reported by many authors [9, 12, 16], and had been associated with the discretization of energy level due to quantum confinement effect [17].

Comparing the electronic band structureof the quantum dots in Figures 6 to 8, it is clear that the highest occupied single-particle state - lowest unoccupied single-particle state (HOMO–LUMO) energy gap decreases with increasing quantum dot size. Apart from this a careful look at Figures 6 and 7 for the Si_5H_{12} and Si_8H_{11} structures shows that the HOMO and LUMO levels are aligned approximately at the $\Gamma(0.0, 0.0, 0.0)$ symmetry point, which is a good indication of a shift from indirect band gap properties as seen for bulk silicon to a direct band gap electronic band structures.

Table 3 shows the calculated band gaps and their corrected values for the different structures studied in this research. A plot of the dependence of the band gap energy on the size of the quantum dot is shown in Figure 9. Although the calculated band gap energy vary around the experimental value of bulk silicon ($1.10eV$), there is a clear band gap energy decrease with increasing particle size. This trend has been established both theoretically and experimentally [18, 19]. The relationship between the band gap energy and the size of the nc-Si can be written as [20];

$E = E_g + \Delta E.$ where E_g the band gap of bulk silicon, and ΔE is the additional energy due to quantum confinement of the electronic states resulting from electrons and holes being squeezed into a dimension that approaches a critical quantum measurement, called the exciton Bohr radius [19, 21]. It is clear from the above that the constructed quantum structures used in this study exihibit quantum confinement effect and their band structure can be engineered by varying the number of the constituent silicon atoms with appropriate dangling bond passivation with hydrogen.

Table 3: Types of Quantum Dot with calculated and corrected band gaps

Molecule	Lattice parameter a_o	Calculated band gap	corrected band gap	Type of band structure
Si_5H_{12}	$5.82\,\mathring{A}$	$1.22eV$	$1.80eV$	Direct
Si_8H_{11}	$7.41\,\mathring{A}$	$0.43eV$	$1.01eV$	Direct
$Si_{16}H_{20}$	$11.13\,\mathring{A}$	$0.15eV$	$0.73eV$	Fairly Direct

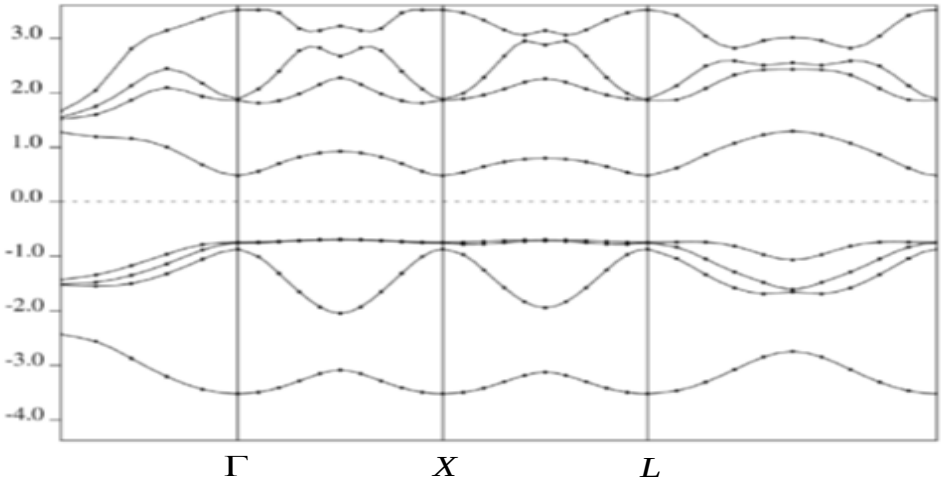

Figure 6: The Variation of Electronic Band Structure with Quantum Dot Size for Si_5H_{12}.

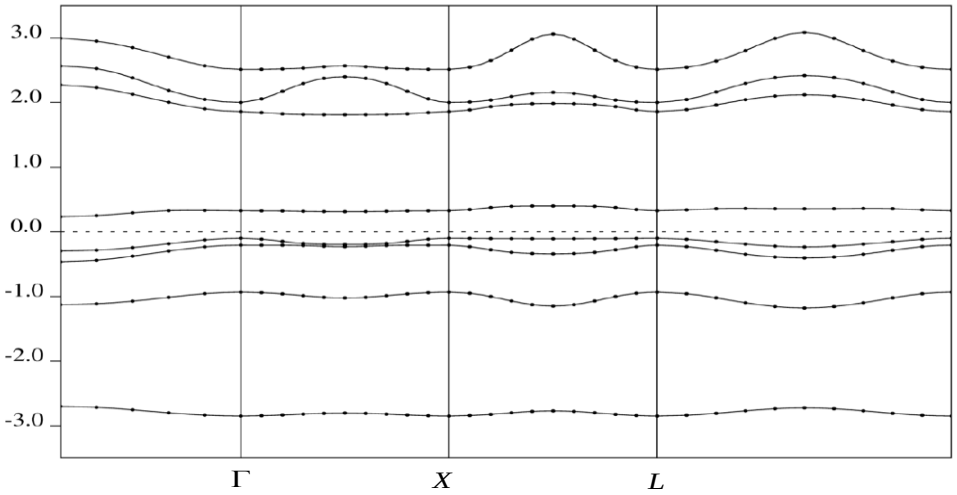

Figure 7: The Variation of Electronic Band Structure with Quantum Dot Size for Si_8H_{11}.

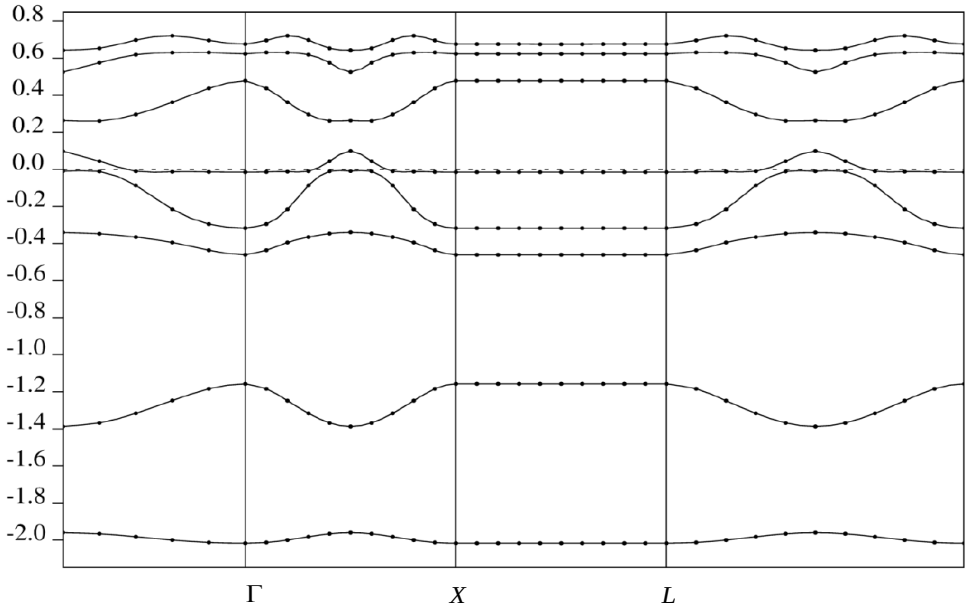

Figure 8: The Variation of Electronic Band Structure with Quantum Dot Size for $Si_{16}H_{20}$.

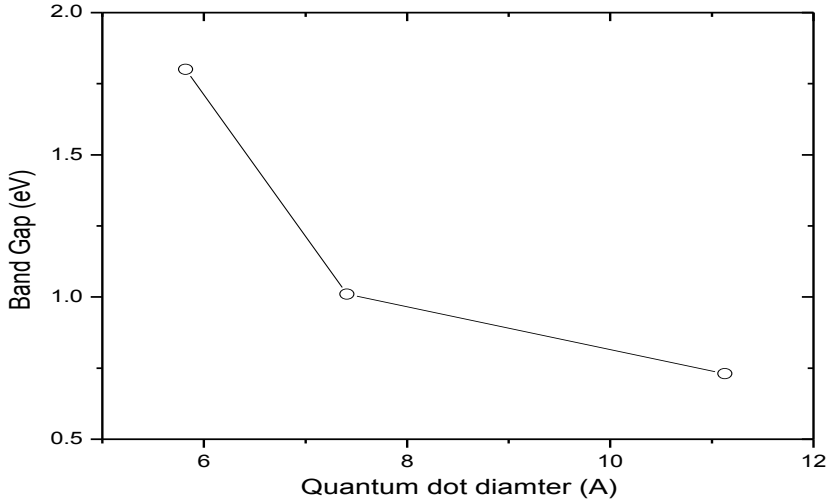

Figure 9: The Variation of Band Gap Energy with Quantum Dot Size.

4.0 Conclusion

Three different supercells of silicon quantum-dots have been constructed consisting of five, eight and sixteen-atoms of silicon, where all the silicon dangling bonds were passivated by hydrogen atoms. The effect of planewave cutoff energy, K–points and lattice constants of silicon quantum dots on the total system energy were investigated based on planewavepseudopotential density functional theory (DFT) method. The numerical values of the bulk modulus, equilibrium volume, equilibrium energy, as well as the equilibrium lattice constants for the three types of silicon quantum dot were derived by fitting the Birch–Murnaghan equation of state to the variation of lattice constants and total system energy. It can be deduced from the study that the Si–Si and Si–H bond lengths are approximately structurally size independent as shown in table 1; whereas the reverse is the case of the bond angles. Also, the lattice constant and the equilibrium volume in each case, increases with an increasing molecular size; whereas the bulk modulus and the equilibrium energy decreases as the size of the silicon quantum dots increases. Thus, the total system energy decreases with increasing planewavecutoff energy, K–points, and lattice constant values.

Furthermore, the result shows distinctively, the discretization of energy levels in the band structure due to quantum confinement effect as the HOMO–LUMO energy gap decreases with increasing quantum dot size. Thus, the HOMO–LUMO alignment in the structures, are good indication of a shift from indirect band gap (for bulk silicon) to a direct gap electronic band structure for quantum dots. Finally, the total system energy obtained in this study follows a similar pattern for three varying parameters; hence it can be used to predict the distribution and shapes of other structures.

Reference

[1] Chih-Hsien Cheng, Yu-Chung Lien, Chung-Lun Wu, and Gong-Ru Li, (2013) *Multicolor electroluminescent Si quantum dots embedded in SiO_X thin film MOSLED with 2.4% external quantum efficiency*, Optics Express, Vol. **21**, Issue 1, pp. 391 – 403.

[2] Stephanie M. Reimann and MattiManninen, (2002) *Electronic structure of quantum dots*, REVIEWS OF MODERN PHYSICS, VOLUME **74**, No. 4, p. 1284.

[3] IlyaSychugov, (2006) *Synthesis properties of single luminescent silicon quantum dots*, Royal Institute of Technology, Doctoral Thesis, Stockholm, Sweden, p. 4-13, 32.

[4] Chemical & Engineering News, (2013) LEDs Made From Silicon Quantum Dots Shine in New Colors, Volume 91, Issue**5**, p. 8.

[5] Yang C. H., Rossi A., Ruskov R., Lai N. S., Mohiyaddin F. A., Lee S., Tahan C., Klimeck G., Morello A., and Dzurak A. S., (2013) *Spin-valley lifetimes in a silicon quantum dot with tunable valley splitting*, http://arxiv.org/pdf/1302.0983v1.pdf, [Cond-mat.mes-hall], p. 1-11.

[6] Florian Maier-Flaig, Julia Rinck, Moritz Stephan, Tobias Bocksrocker, Michael Bruns, Christian Kübel, Annie K. Powell, Geoffrey A. Ozin and UliLemmer, (2013) *Multicolor Silicon Light-Emitting Diodes (SiLEDs)*, American Chemical Society, Nano-letters, **13**(2), p. 475–480.

[7] Chih-Hsien Cheng, Yu-Chung Lien, Chung-Lun Wu, and Gong-Ru Lin, (2013) *Multicolor electroluminescent Si quantum dots embedded in SiO_X thin film MOSLED with 2.4% external quantum efficiency*, Optics Express, Vol. **21**, Issue 1, p. 391 – 403.

[8] Ioannou-Sougleridis V., Ouisse T., Nassiopoulou A. G., Bassani F. and Arnaud d'Avitaya F., (2001) *Nonlinear electrical transport in nc-Si/CaF_2 multilayer structures with ultrathin CaF_2 layers*, Journal of Applied Physics, Vol. **89**, No 1, p.610.

[9] Gong, X.G., (1995) *Stability and electronic properties of nanoscale silicon cluster.* Physical Review B, **52** (20): p. 677 - 681.

[10] Sholl, D.S. and J.A. Steckel, (2009): *Density Functional Theory, Apractical Introduction.*: John Wiley and Sons Inc.

[11] Kilian, K.A., D.A. Drabold, and J.B. Adams, (1993) *First-principles simulation of a-Si and a-Si:H surfaces.* Physical Review B,**48**(23): p. 393 - 399.

[12] Du, J. and P. Kroll, (2010) *Electronic stucture and interfacial properties of Ge nanoclusters embedded in amorphous silica.* Journal of Non-Crystalline Solids, 2010. **356**: p. 2448 - 2453.

[13] Liang, L., H. Ma, and Y. Wei, (2011) *Size-Dependent Elastic Modulus and Vibration Frequency of Nanocrystals.* Journal of NanomaterialsVolume, **6**: p. pages doi:10.1155/2011/670857.

[14] Yadav, A.S., et al., (2006) *Ab initio study of silicon in GW approximation: A direct band gap semiconductor.* Progress in crystal growth and characterisation of materials,**52**: p. 10 -14.

[15] Godby, R.W., M. Schluter, and L.J. Sham, (1986) Physical Review Letters,**56** (22): p. 2415 - 2418.

[16] Iori, F., et al., (2008) *Novel optoelectronic properties of simultaneously n- and p-doped silicon nanostructures.* Superlattices and Microstructures, **44**: p. 337-347.

[17] Odo, E.A., (2009) *Synthesis, characterisation and device applications of silicon nanoparticles produced by mechanical attrition*, University of Cape Town: Cape Town.

[18] Zhao, X., et al., (1994)*Quantum confinement in nanometer-sized silicon crystallites.* Phys. Rev. B, **50**(24): p. 18654-18657.

[19] YOFFE, A.D., (1993)*Low dimensional syatems: quantisation effect and electronic properties of semiconductor microcrystallites (Zero-dimensional systems) and some quasi-two-dimensional systems.* ADVANCES IN PHYSICS, **42**(2): p. 173 - 266.

[20] Kelsall, R., I. Hamley, and M. Geoghegan, (2005)*Nanoscale Science and Technology*. Jonh Wiley and Sons Ltd.

[21] Ngage, R., (2008)*Quantum Dots*. Available from: http://www.waterengage.com/researchwiki/index.php?title=Quantum_Dots.